# The sensitivity of the El Niño- Indian monsoon teleconnection to Maritime Continent cold SST anomalies

Umakanth Uppara[1,4]*, Ben Webber[1], Manoj Joshi[1], Andrew Turner[2,3]

[1]Climatic Research Unit, School of Environmental Sciences, University of East Anglia, Norwich, NR4 7TJ, UK

[2]Department of Meteorology, University of Reading, Reading, RG6 6ET, UK

[3]National Centre for Atmospheric Sciences, University of Reading, Reading, RG6 6ES, UK

[4]BK21 School of Earth Environmental Systems, Pusan National University, Busan, 46241, Republic of Korea

*Correspondence to: umakanth@pusan.ac.kr

## Key points

- The distribution of cold SSTs around the Maritime Continent strongly influences the Indian Summer Monsoon during eastern Pacific El Niños
- The ISM response is strongly modulated by the regional meridional circulation in response to changes in SST.
- Teleconnection pathways to the ISM from regions of SST anomalies combine in a non-linear way.

## Abstract

The study investigates how sea surface temperature (SST) anomalies surrounding the Maritime Continent (MC) modulate the impact of developing El Niño events on Indian Summer Monsoon (ISM) rainfall. Using a climate model we find that the ISM rainfall response to tropical Pacific SST anomalies of eastern and central Pacific El Niño events is sensitive to the details of cold SST anomalies surrounding the MC. Furthermore, the remote rainfall responses to regions of SST anomalies do not combine linearly and depend strongly on gradients in the SST anomaly patterns. The cold SST anomalies around the MC have a significantly larger impact on the ISM response to eastern Pacific events than to central Pacific events. These results show the usefulness of idealised modelling experiments, which offer insights into the complex interactions of the ISM with modes of climate variability.

## Plain Language Summary

El Niño events often coincide with droughts in the Indian subcontinent, though the correlation is far from perfect, partially due to the so-called Indian Ocean Dipole (IOD). A climate model driven by idealised combinations of SST anomalies is used to examine the combined influence of different El Niño events and the IOD on the summer monsoon. We find that the effect of these events on monsoon drought is particularly sensitive to the patterns of SST around the Maritime Continent region, especially during El Niño events that occur in the far-east Pacific. These results show the importance of idealised modelling experiments that can often tease apart complex interactions in a way that individual state-of-the-art model runs cannot.

## 1. Introduction

The El Niño Southern Oscillation (ENSO) originates in the tropical Pacific Ocean, and its remote influence on ISM variability and rainfall has been widely investigated, often leading to droughts during the developing phase of ENSO events (Rasmusson and Carpenter, 1983; Ju and Slingo, 1995; Kripalani and Kulkarni, 1997; Soman and Slingo, 1997; Webster et al., 1998). The eastward shift of the Walker circulation during the developing phase of an El Niño event causes anomalous subsidence of air in the Western Pacific (WP) and over the Indian subcontinent, resulting in a decrease in ISM rainfall (Goswami, 1998; Kumar et al., 1999; Lau and Wang, 2006). Adding to the complexity is decadal variability in the teleconnection patterns (e.g., Fan et al., 2021) and the presence of different types of El Niño events: Eastern-Pacific (EP) El Niño events are characterized by warm SST anomalies in the eastern equatorial Pacific, while Central-Pacific (CP) events are characterized by warm SST anomalies over the central Pacific (Trenberth and Stepaniak, 2001; Ashok et al., 2007; Kao and Yu, 2009; Kug et al., 2009; Yeh et al., 2009). Kumar et al. (2006) suggested that CP events play an important role in the ISM teleconnection, causing more severe drought conditions over India than EP events.

The circulation over the WP, and the teleconnection from ENSO to the ISM, are strongly influenced by SST anomalies over the Indian Ocean, and by central or eastern Pacific warm SST anomalies during the developing phase of El Niño (e.g., Wang et al., 2003; Chen et al., 2007, He et al., 2020). WP cooling and the associated non-linear atmospheric response is thought to be important for the asymmetric duration of El Niño and La Niña events (e.g., Okumura et al., 2011). It has been suggested that the presence of an IOD event (Indian Ocean Dipole, Saji et al., 1999) impacts convective activity over the south-east Indian Ocean region (SEIO) and the WP during the developing phase of an El Niño event (Annamalai et al., 2005) and that IOD events can reduce the impact of co-occurring ENSO events on the ISM rainfall (Behera et al., 1999; Li et al., 2003; Saji and Yamagata, 2003; Ashok et al., 2004; Cherchi et al., 2007; Cherchi and Navarra, 2013). Jang and Straus (2012) studied the influence of adding heating/cooling over the maritime continent (MC) to weaken or strengthen the ISM during the developing phase of the 1987 El Niño, showing anticyclonic/cyclonic anomalies extending over India in response to MC heating/cooling, respectively.

Despite these advances, the relationship between ENSO and the ISM is a challenging problem because of the complex nature of its numerous coupled interactions. In this study an effort is made to tease apart such interactions with a series of idealized model experiments using an atmosphere-only General Circulation Model (GCM) forced by a range of possible SST patterns associated with EP and CP El Niño types. We isolate the effects of cold SSTs across the MC on ISM rainfall during the development of El Niño and study their interaction with warm SST anomalies in the central and eastern Pacific. A description of the model and experiments is given in Section 2. The results of the simulations are shown in Section 3, followed by discussion in Section 4 and conclusions in Section 5.

## 2. Methods

The IGCM4 (Intermediate Global Circulation Model version 4; Joshi et al., 2015) used in this study is a global spectral atmospheric model with a standard configuration of T42L20, i.e., 128 × 64 grid points in the horizontal and 20 layers in the vertical. This configuration of the model has been used extensively in atmospheric and climate research (e.g., Joshi et al., 2015; van der Wiel et al., 2016; Ratna et al., 2020, 2021). Its speed and flexibility make it well-suited for idealized experiments. It has simpler parameterization schemes for physical processes such as convective and boundary-layer mixing than state-of-the-art GCMs (see Joshi et al., 2015). Land surface temperatures and soil moisture are allowed to evolve self-consistently with the GCM using a two-layer model of the soil (Forster et al., 2000). SSTs in the control run are imposed as a seasonally varying climatology (calculated over 1971-2000) of skin temperature obtained from NOAA-CIRES Twentieth Century Reanalysis Version 3 (Compo et al., 2011).

SST anomaly composites of ENSO and IOD events are added to the control SSTs for the perturbation experiments (see Text S1). A set of 10 model sensitivity experiments (listed in Table 1 & Table S1) are conducted by imposing SST anomalies in the Indian and Pacific Ocean basins, as shown in Figure 1 & S1. The model starts from rest and is integrated for 35 years, the first five years of which are discarded to account for any model spin-up. Runs “EP” and “CP” refer to the full EP and CP Pacific SST anomalies respectively (Fig. 1 c-d), while subscripts “W” and “C” respectively refer to runs containing only the warm (Fig. 1 a-b) or cold (Fig. S1 a-b) components of the Pacific SST anomaly fields. The same subscripts are used for IOD SST anomalies, so for

example, EP+$I_C$ represents the whole-basin EP SST anomalies in the Pacific, combined with the cold SEIO SST anomalies associated with the IOD in the Indian Ocean (Fig. 1 e-f), while $EP_C$+$I_C$ represents only the cold anomalies in the EP runs, combined with cold SEIO SSTs associated with the IOD (Fig. S1c-d).

In the control experiment, the model simulates ISM rainfall well, despite overestimation of rainfall amounts over the northern Bay of Bengal (BoB) and the WP (Figure S2). This ISM wet bias contrasts with the typical large ISM dry bias found in CMIP-class models (Sperber et al., 2013). Circulation biases are consistent with these rainfall biases, e.g., low-level wind biases include southerly flow across the equator over the central and eastern Indian Ocean (IO and westerlies over the WP), while at the upper levels wind biases include easterly flow over the MC and WP (see Figure S2).

## 3. Results

Figure 2 shows the JJAS mean rainfall and low-level 850 hPa circulation response to SST anomalies in the model experiments. All runs display reductions in rainfall over the ISM and enhanced rainfall (associated with cyclonic circulation anomalies) in the southern Indian Ocean east of Madagascar, as well as over the Philippines. However, interesting differences do exist in the magnitude and extent of these anomalies. As an example, the difference in rainfall response over India between EP and EP+Ic is quite sizeable, whereas the difference in the rainfall response over India between CP and CP+Ic is small. In contrast, the difference in rainfall response over India between EP and $EP_W$ is quite small, whereas the difference in the rainfall response over India between CP and $CP_W$ is larger. In addition, the cyclonic anomaly east of Madagascar is more intense with larger zonal extent in $CP_W$ compared with CP. The differences can only be in response to the differences in the magnitude and the location of warming (Fig. 1a-b) as well as its spatial distribution.

The atmospheric response to each set of SST forcings can be better understood by examining the velocity potential and divergent winds in the upper and lower troposphere (Fig. 3 & S4). The upper-level convergence (associated with anomalous subsidence) corresponding to the reduction

in rainfall is striking over the ISM region. In EP (Fig. 3b) there are three centres of anomalous subsidence located over the Indian subcontinent, equatorial east Africa, and the Maritime Continent. However, in CP (Fig. 3d) anomalous subsidence is relatively weak but appears over a wider region enclosing the north Indian Ocean. When considering the warm component of the SSTs only, the divergence patterns of $EP_w$ and EP are quite similar- but those of $CP_w$ and CP are very different, with $CP_w$ exhibiting a much stronger anomalous convergence over the western IO, suggesting that the ISM response to western Pacific cold anomalies depends on whether the developing El Niño is a CP or EP type.

The sensitivity of the ISM response to cold SST anomalies associated with the IOD is also apparent from Figure 3. When including such anomalies, the divergence patterns in EP+Ic and CP+Ic are very different to the patterns of EP and CP respectively, as is known from previous work that shows the dependence of ISM response on the sign of the IOD and that IOD events can reduce the impact of co-occurring ENSO events (Behera et al., 2006; Ashok et al., 2004; Shinoda et al., 2004;; Lee Drbohlav et al., 2007; Cherchi and Navarra, 2013). However, our results demonstrate that, for EP events, the cold SSTs in the SEIO region are sufficient to substantially reduce the rainfall over India, while for CP events there is relatively little difference in the ISM region. We consider possible reasons for these differences in the Discussion.

It is known that regional teleconnections from El Niño not only depend on the magnitude of the SST anomalies, but also on their gradients (e.g., Trenberth and Stepaniak 2001). Accordingly, we have calculated the JJAS SST gradient between Niño4 (5°S-5°N, 160°E-150°W) and the northwest Pacific region (0-10°N, 130°E-150°E) as suggested by Hoell and Funk (2013), and there is no significant difference in the SST gradient values in EP (0.61°C) and CP (0.59°C) respectively. However, there are differences in the spatial distribution of these cold SST anomalies over WP (Fig. S1a-b). Therefore, a pair of model experiments $EP_C$ and $CP_C$ are conducted by forcing with WP cold SST anomalies alone. The ISM response is very weak in $CP_C$ (Fig. S3a-b), which could be one of the possible reasons for no significant difference between EP and $EP_W$. We return to the potential importance of SST gradients in the Discussion.

Given the sensitivity of the model response to relatively small-scale SST anomalies, we use the additional $EP_C+I_C$ and $CP_C+I_C$ (Fig. S1c-d) runs to investigate the degree of non-linearity in the model responses to the addition of cold SST anomalies over the WP and MC regions. Fig. 4 shows the rainfall response to the sum of SST anomalies, compared to the sum of the rainfall responses to individual SST anomalies. Fig. 4a for instance examines the difference between the response in EP (Pacific basin-wide cold and warm SST anomalies) with the sum of the responses in $EP_W$ (warm anomalies only) and $EP_C$ (cold anomalies only).

The positive rainfall anomaly over India in Fig. 4a and its further enhancement in Fig. 4c can be attributed to the non-linear interactions arising from the combined SST forcing. The strong ISM response in Figure 4c (well over 1 $mmd^{-1}$) shows the nonlinearity in response to cold and warm SST anomalies in the Pacific Ocean during a developing EP El Niño, as the reduction in ISM rainfall when considering cold and warm SST anomalies separately is much lower than considering the whole basin-wide SST anomaly field. In contrast, a dipole exists in ISM rainfall in Fig. 4b, suggesting that during a developing CP El Niño, the response of ISM rainfall when considering cold and warm SST anomalies separately is somewhat higher than considering the whole basin-wide SST anomaly field. The nonlinearity is reflected in the 200 hPa anomalous wind divergence pattern (Fig. S5), which shows divergent wind anomalies over large parts of Southeast Asia.

## 4. Discussion

The response to anomalous warm and cold SST forcing can be understood as a combination of shifts in zonal and meridional circulation cells and equatorial Rossby waves forced by the anomalous deep convection and latent heat release. The Rossby wave response is clear in Fig. 2, with enhanced rainfall extending west of the dateline around 15°N and 15°S. This enhanced rainfall coincides with local cold SST anomalies, emphasising that this is a remote response to the central and eastern Pacific warm SSTs. In the $EP_W$ simulations (Fig. 2a), the positive rainfall and cyclonic circulation anomalies associated with this Rossby wave signal extends into southeast Asia and is consistent with westerly anomalies strengthening the monsoon winds over the Bay of Bengal that would create additional low-level divergence and reinforce drying over parts of India. In $CP_W$ (Fig. 2b), this enhanced rainfall is slightly further north, the low-level wind anomalies over the

Bay of Bengal are weaker, and the anomalies over the ISM are weaker. Therefore, there appears to be a relationship between the strength of the rainfall anomalies over Southeast Asia, in turn a remote Rossby wave response to the eastern Pacific warm SSTs, and the magnitude and location of the dry anomalies over the Indian subcontinent.

All simulations demonstrate a clear shift in the strength and location of the Walker circulation, as shown by the upper-level divergent winds and velocity potential (Fig. 3). This is stronger for EP and $EP_W$ than for CP and $CP_W$ (compare Fig. 3 a,c with Fig. 3 b,d), which may be due to the larger magnitude of the SST anomalies for EP events than CP events (Fig. 1 c,d). The upper-level anomalous convergence extends from the MC region over the Bay of Bengal to the Indian Subcontinent. There is also an anomalous meridional circulation cell evident over the western Indian Ocean, with upper-level convergent (divergent) wind anomalies over the northern (southern) IO, which form the descending (rising) branch of a local meridional overturning circulation that opposes the mean circulation of the monsoon and thus contributes to the drying over India (Figs. 2, 3). However, while the strength of this meridional circulation varies between the experiments, it is difficult to robustly link this to the SST forcing applied.

The addition of cold SST anomalies in the SEIO region markedly reduces the magnitude of the velocity potential anomalies for $EP+I_C$ compared with EP. The rainfall anomalies for these two simulations are strikingly different over the Bay of Bengal and central India, consistent with much weaker wind anomalies here in $EP+I_C$ (Fig. 2 c,e). The low-level divergent winds are also weaker here (Fig. S4 c,e), likely because the low-level outflow from the reduced rainfall over the SEIO counters the monsoon winds over the Bay of Bengal. As a result, the rainfall anomalies over the Bay of Bengal are weaker, which may lead to further feedbacks on the regional circulation anomalies. In contrast, for CP events, the enhanced rainfall over Southeast Asia is consistent with stronger low-level divergent winds over the Bay of Bengal, contributing to an anomalous zonal circulation cell and thus amplifying the dry anomalies over India.

The ISM response to a developing El Niño event appears to be as sensitive to the nature of cold SST anomalies around the MC as it is to the actual type of El Niño event underway. For example, the difference in rainfall over Southeast Asia between $EP+I_C$ and $CP+I_C$ may be due to

the meridional SST gradients around the MC, since for CP+$I_C$ (Fig. 1f), the cooling is much more pronounced to the south of the MC than to the north, while this meridional gradient is weaker for EP+$I_C$ (Fig. 1e). However, we note that the response to the cold SSTs alone (Fig. S3) is very different to the response to combined warm and cold SSTs, underlining the importance of non-linear combinations of local and remote responses. This non-linearity, combined with the high sensitivity to small details in the SST patterns, increases the difficulty of interpreting the rainfall response to individual ENSO and IOD events. Previous research has identified the high sensitivity of the atmosphere to small SST perturbations over the West Pacific warm pool (Ju and Slingo, 1995), arising from the non-linear nature of the Clausius-Clapeyron relationship and very warm climatological SSTs in the region. The responses shown above indicate that the details of the SST gradients are at least as important as the location and magnitude of individual SST patterns in determining the remote response, in agreement with previous studies (e.g., Hoell and Funk, 2013; Karnauskas et al., 2009; Vera et al., 2004).

The IGCM experiments focussing on distinguishing the response to combinations of SST patterns add new understanding to the existing knowledge on relationships between El Niño and the ISM, emphasising the importance of SST anomalies and SST gradients in the vicinity of the MC. Our idealised experiments necessarily include some simplifications. IGCM4 is an atmosphere-only model, so there are no feedbacks from ocean-atmosphere interactions. Such feedbacks are known to lead to markedly different results in coupled models compared with atmosphere-only simulations (Kumar et al., 2005). Negative feedbacks from cloud-cover on SST could reduce the magnitude of the tropical convection response to SST anomalies. However, using an atmosphere-only model is necessary to precisely specify the SST patterns such that they resemble composite anomalies, and has the benefit of avoiding the ocean biases that exist in most coupled models.

## 4. Conclusions

We have used a simplified GCM (IGCM4) to investigate how ISM rainfall and circulation respond to SST anomalies associated with EP and CP El Niño events, separated into their warm and cold SST components, and in combination with cold SST components of IOD events. A key

result of our study is that the cold SST anomalies around the Maritime Continent strongly modulate the teleconnection from warm developing El Niño SST anomalies in the central and eastern Pacific. Warm Pacific SST anomalies alone do produce a strong response in the ISM region, but this is strengthened and modified by the addition of the cold WP SSTs and the associated stronger zonal SST gradients in a manner that is non-linear and not a simple superposition of anomalies. When the Pacific warm anomalies are combined with cold SSTs anomalies around the MC (i.e., cold SSTs over WP and SEIO), the influence on the ISM rainfall and the circulation is more significantly reduced in EP compared with CP El Niño events.

Differences in SST gradients create important local differences in divergence patterns that induce remote responses and feedbacks. The non-linear interaction of Indian and Pacific SST forcings as well as the importance of small-scale details and SST gradients in individual basins hamper efforts to define a simple conceptual model of the ISM response to ENSO and the IOD. The importance of accurately simulating such small-scale details presents a substantial challenge for coupled ocean-atmosphere climate modelling, especially because of the complex topography and island morphology in this region. Studying the individual responses of the ISM to ENSO and IOD SST forcings is undoubtedly useful, but studying combinations is crucial to determining and understanding the full response. Small differences in SST patterns and associated gradients can have substantial impacts on ISM precipitation anomalies, which may contribute to the observed variability in the ISM response to ENSO events, and as such are worthy of further research.

## Acknowledgements

The research presented here arose from the STIMULATE project and was funded under the Met Office Weather and Climate Science for Services Partnership (WCSSP) India Programme. This research was carried out on the High-Performance Computing Cluster supported by the Research and Specialist Computing Support service at the University of East Anglia.

## Data Availability Statement

The data used in this study can be downloaded from the following websites:

GPCP (https://psl.noaa.gov/data/gridded/data.gpcp.html);

NOAA-CIRES V2c (https://psl.noaa.gov/data/gridded/data.20thC_ReanV2c.html)

IGCM used is described in Joshi et al. (2015; https://gmd.copernicus.org/articles/8/1157/2015/)

**References**


Annamalai, H., S. P. Xie, and J. P. McCreary (2005), Impact of Indian Ocean Sea surface temperature on developing El Niño, J. Clim., 18, 302– 319. https://doi.org/10.1175/JCLI-3268.1

Ashok, K., Behera, S. K., Rao, S. A., Weng, H., & Yamagata, T. (2007). El Niño Modoki and its possible teleconnection. Journal of Geophysical Research: Oceans, 112(11). https://doi.org/10.1029/2006JC003798

Ashok, K., Guan, Z., Saji, N. H., & Yamagata, T. (2004). Individual and combined influences of ENSO and the Indian Ocean Dipole on the Indian summer monsoon. Journal of Climate, 17(16), 3141–3155. https://doi.org/10.1175/1520-0442(2004)017<3141:IACIOE>2.0.CO;2

Behera, S. K., Krishnan, R., & Yamagata, T. (1999). Unusual ocean-atmosphere conditions in the tropical Indian Ocean during 1994. Geophysical Research Letters, 26(19), 3001–3004. https://doi.org/10.1029/1999GL010434

Behera, S. K., Luo, J. J., Masson, S., Rao, S. A., Sakuma, H., & Yamagata, T. (2006). A CGCM study on the interaction between IOD and ENSO. Journal of Climate, 19(9), 1688–1705. https://doi.org/10.1175/JCLI3797.1

Chen, J. M., Li, T., & Shih, C. F. (2007). Fall persistence barrier of sea surface temperature in the South China Sea associated with ENSO. Journal of Climate, 20(2), 158–172. https://doi.org/10.1175/JCLI4000.1

Cherchi, A., & Navarra, A. (2013). Influence of ENSO and of the Indian Ocean Dipole on the Indian summer monsoon variability. Climate Dynamics, 41(1), 81–103. https://doi.org/10.1007/s00382-012-1602-y

Cherchi, A., Gualdi, S., Behera, S., Luo, J. J., Masson, S., Yamagata, T., & Navarra, A. (2007). The influence of tropical Indian Ocean SST on the Indian summer monsoon. In Journal of Climate, 20(13), 3083–3105. https://doi.org/10.1175/JCLI4161.1

Compo, G. P., Whitaker, J. S., Sardeshmukh, P. D., Matsui, N., Allan, R. J., Yin, X., et al. (2011). The Twentieth Century Reanalysis Project. Quarterly Journal of the Royal Meteorological Society,137(654),1-28. https://doi.org/10.1002/qj.776

Fan, F., Lin, R., Fang, X., Xue, F., Zheng, F., & Zhu, J. (2021). Influence of the Eastern Pacific and Central Pacific Types of ENSO on the South Asian Summer Monsoon. Advances in Atmospheric Sciences, 38(1), 12–28. https://doi.org/10.1007/s00376-020-0055-1

Forster, P. M. D. F., Blackburn, M., Glover, R., & Shine, K. P. (2000). An examination of climate sensitivity for idealised climate change experiments in an intermediate general circulation model. Climate Dynamics, 16(10–11), 833–849. https://doi.org/10.1007/s003820000083

Goswami, B. N. (1998). Interannual variations of Indian summer monsoon in a GCM: external conditions versus internal feedbacks. Journal of Climate, 11(4), 501–522. https://doi.org/10.1175/1520-0442(1998)011<0501:IVOISM>2.0.CO;2

He, S., Yu, J. Y., Yang, S., & Fang, S. W. (2020). ENSO's impacts on the tropical Indian and Atlantic Oceans via tropical atmospheric processes: observations versus CMIP5 simulations. Climate Dynamics, 54(11), 4627-4640. https://doi.org/10.1007/s00382-020-05247-w

Hoell, A., & Funk, C. (2013). The ENSO-related West Pacific Sea surface temperature gradient. Journal of Climate, 26(23), 9545–9562. https://doi.org/10.1175/JCLI-D-12-00344.1

Jang, Y., & Straus, D. M. (2012). The Indian monsoon circulation response to El Niño diabatic heating. Journal of Climate, 25(21), 7487–7508. https://doi.org/10.1175/JCLI-D-11-00637.1

Joshi, M., Stringer, M., Van Der Wiel, K., O'Callaghan, A., & Fueglistaler, S. (2015). IGCM4: A fast, parallel and flexible intermediate climate model. Geoscientific Model Development, 8(4), 1157–1167. https://doi.org/10.5194/gmd-8-1157-2015

Ju, J., & Slingo, J. (1995). The Asian summer monsoon and ENSO. Quarterly Journal of the Royal Meteorological Society, 121(525), 1133–1168. https://doi.org/10.1002/qj.49712152509

Kao, H. Y., & Yu, J. Y. (2009). Contrasting Eastern-Pacific and Central-Pacific types of ENSO. Journal of Climate, 22(3), 615–632. https://doi.org/10.1175/2008JCLI2309.1

Karnauskas, K. B., Seager, R., Kaplan, A., Kushnir, Y., & Cane, M. A. (2009). Observed strengthening of the zonal sea surface temperature gradient across the equatorial Pacific Ocean. *Journal of Climate*, *22*(16), 4316–4321. https://doi.org/10.1175/2009JCLI2936.1

Kripalani, R. H., & Kulkarni, A. (1997). Climatic impact of El Niño/La Niña on the Indian monsoon: A new perspective. Weather, 52(2), 39–46. https://doi.org/10.1002/j.1477-8696.1997.tb06267.x

Kug, J. S., Jin, F. F., & An, S. Il. (2009). Two types of El Niño events: Cold tongue El Niño and warm pool El Niño. Journal of Climate, 22(6), 1499–1515. https://doi.org/10.1175/2008JCLI2624.1

Kumar, K. K., Rajagopalan, B., & Cane, M. A. (1999). On the weakening relationship between the Indian monsoon and ENSO. Science, 284(5423), 2156–2159. https://doi.org/10.1126/science.284.5423.2156

Kumar, K. K., Hoerling, M., & Rajagopalan, B. (2005). Advancing dynamical prediction of Indian monsoon rainfall. Geophysical Research Letters, 32, L08704. https://doi.org/10.1029/2004GL021979

Kumar, K. K., Rajagopalan, B., Hoerling, M., Bates, G., & Cane, M. (2006). Unraveling the mystery of Indian monsoon failure during El Niño. Science, 314(5796), 115–119. https://doi.org/10.1126/science.1131152

Lau, N.-C., & Wang, B. (2006). Interactions between the Asian monsoon and the El Niño/Southern Oscillation. In The Asian Monsoon (pp. 479–512). https://doi.org/10.1007/3-540-37722-0_12

Lee Drbohlav, H. K., Gualdi, S., & Navarra, A. (2007). A diagnostic study of the Indian Ocean dipole mode in El Niño and non-El Niño years. In Journal of Climate, 20(13), 2961–2977. https://doi.org/10.1175/JCLI4153.1

Li, T., Wang, B., Chang, C. P., & Zhang, Y. (2003). A theory for the Indian Ocean dipole-zonal mode. Journal of the Atmospheric Sciences, 60(17), 2119–2135. https://doi.org/10.1175/1520-0469(2003)060<2119:ATFTIO>2.0.CO;2

Okumura, Y. M., & Deser, C. (2010). Asymmetry in the duration of El Niño and La Niña. Journal of Climate, 23(21), 5826– 5843. https://doi.org/10.1175/2010JCLI3592.1

Rasmusson, E. M., & Carpenter, T. H. (1983). The relationship between eastern equatorial Pacific sea surface temperatures and rainfall over India and Sri Lanka. Monthly Weather Review, 111(3), 517–528. https://doi.org/10.1175/1520-0493(1983)111<0517:TRBEEP>2.0.CO;2

Ratna, S. B., Osborn, T. J., Joshi, M., & Luterbacher, J. (2020). The influence of Atlantic variability on Asian summer climate is sensitive to the pattern of the sea surface temperature anomaly. Journal of Climate, 33(17), 7567-7590. https://doi.org/10.1175/JCLI-D-20-0039.1

Ratna, S. B., Cherchi, A., Osborn, T. J., Joshi, M., & Uppara, U. (2021). The Extreme Positive Indian Ocean Dipole of 2019 and Associated Indian Summer Monsoon Rainfall Response. Geophysical Research Letters, 48(2). https://doi.org/10.1029/2020GL091497

Saji, N. H., Goswami, B. N., Vinayachandran, P. N., & Yamagata, T. (1999). A dipole mode in the tropical Indian Ocean. Nature, 401(6751), 360–363. https://doi.org/10.1038/43854

Saji, N. H., & Yamagata, T. (2003). Structure of SST and surface wind variability during Indian Ocean Dipole mode events: COADS observations. Journal of Climate, 16(16), 2735–2751. https://doi.org/10.1175/1520-0442(2003)016<2735:SOSASW>2.0.CO;2

Shinoda, T., Alexander, M. A., & Hendon, H. H. (2004). Remote response of the Indian Ocean to interannual SST variations in the tropical Pacific. Journal of Climate, 17(2), 362–372. https://doi.org/10.1175/1520-0442(2004)017<0362:RROTIO>2.0.CO;2

Soman, M. K., & Slingo, J. (1997). Sensitivity of the Asian summer monsoon to aspects of sea-surface-temperature anomalies in the tropical Pacific Ocean. Quarterly Journal of the Royal Meteorological Society, 123(538), 309–336. https://doi.org/10.1256/smsqj.53803

Sperber, K. R., Annamalai, H., Kang, I. S., Kitoh, A., Moise, A., Turner, A., et al. (2013). The Asian summer monsoon: An intercomparison of CMIP5 vs. CMIP3 simulations of the late 20th century. Climate Dynamics, 41(9–10), 2711–2744. https://doi.org/10.1007/s00382-012-1607-6

Trenberth, K. E., & Stepaniak, D. P. (2001). Indices of El Niño evolution. Journal of Climate, 14(8), 1697–1701. https://doi.org/10.1175/1520-0442(2001)014<1697:LIOENO>2.0.CO;2

van der Wiel, K., Matthews, A. J., Joshi, M. M., & Stevens, D. P. (2016). The influence of diabatic heating in the South Pacific Convergence Zone on Rossby wave propagation and the mean flow. Quarterly Journal of the Royal Meteorological Society, 142(695), 901–910. https://doi.org/10.1002/qj.2692

Vera, C., Silvestri, G., Barros, V., & Carril, A. (2004). Differences in El Niño response over the Southern Hemisphere. *Journal of Climate, 17*(9), 1741–1753. https://doi.org/10.1175/1520-0442(2004)017<1741:DIENRO>2.0.CO;2

Wang, B., Wu, R., & Li, T. (2003). Atmosphere-warm ocean interaction and its impacts on Asian-Australian monsoon variation. Journal of Climate, 16(8), 1195–1211. https://doi.org/10.1175/1520-0442(2003)16<1195:AOIAII>2.0.CO;2

Webster, P. J., Magaña, V. O., Palmer, T. N., Shukla, J., Tomas, R. A., Yanai, M., & Yasunari, T. (1998). Monsoons: processes, predictability, and the prospects for prediction. Journal of Geophysical Research: Oceans, 103(C7), 14451–14510. https://doi.org/10.1029/97jc02719

Yeh, S. W., Kug, J. S., Dewitte, B., Kwon, M. H., Kirtman, B. P., & Jin, F. F. (2009). El Niño in a changing climate. Nature, 461(7263), 511–514. https://doi.org/10.1038/nature08316

## Figures

**Figure 1.** The JJAS mean composites of SST anomalies overlaid with SST climatology to provide surface forcing in IGCM model experiments for EP, CP. In our naming convention, EP and CP suggest whole Pacific-basin SST anomalies, while W and C subscripts indicate experiments in which only the warm or cold SST anomalies are retained (respectively) for El Niño (over Pacific Ocean) and IOD (over Indian Ocean) events.

**Figure 2.** IGCM responses in JJAS rainfall (shaded, mm $d^{-1}$) and circulation (850 hPa wind vectors; m $s^{-1}$) over the ISM domain for the 6 model experiments shown in Figure 1. (**a-b**) the model response to Pacific warm SST forcing only ($EP_W$, $CP_W$); **(c-d)** model response to whole-basin SST forcing (EP, CP); **(e-f)** model response to EP, CP SSTs combined with cold Indian Ocean SST anomalies associated with IOD events ($EP+I_C$, $CP+I_C$). The wind vectors (black) and the precipitation (hatched) represent statistical significance at the 90% confidence level based on a student's t-test.

**Figure 3.** Same as Figure 2, but for upper level (200 hPa) velocity potential (shaded; $10^{-6}$, $m^2$ $s^{-1}$) overlaid with divergent wind anomalies (vectors). Only signals of velocity potential significant at the 90% level are shown (shaded), while divergent winds are shaded grey (black) below (above) this level.

**Figure 4.** Non-linearity in IGCM responses to SST forcing during JJAS, (a-b) rainfall (shaded, mm $d^{-1}$) and circulation (850 hPa wind vectors; m $s^{-1}$) responses between EP (CP) and the sum of responses to $EP_W$ and $EP_C$ ($CP_W$ and $CP_C$), (c-d) between $EP+I_C$ ($CP+I_C$) and the sum of responses to $EP_W$ and $EP_C+I_C$ ($CP_W$ and $CP_C+I_C$).

## Tables

**Table 1**: The list of model experiments. In our naming convention, EP and CP suggest whole Pacific basin SST anomalies, while 'W' and 'C' subscripts indicate experiments where only the

warm or cold SST anomalies are retained (respectively) for El Niño (over Pacific Ocean) and IOD (over Indian Ocean) events.

## Figures

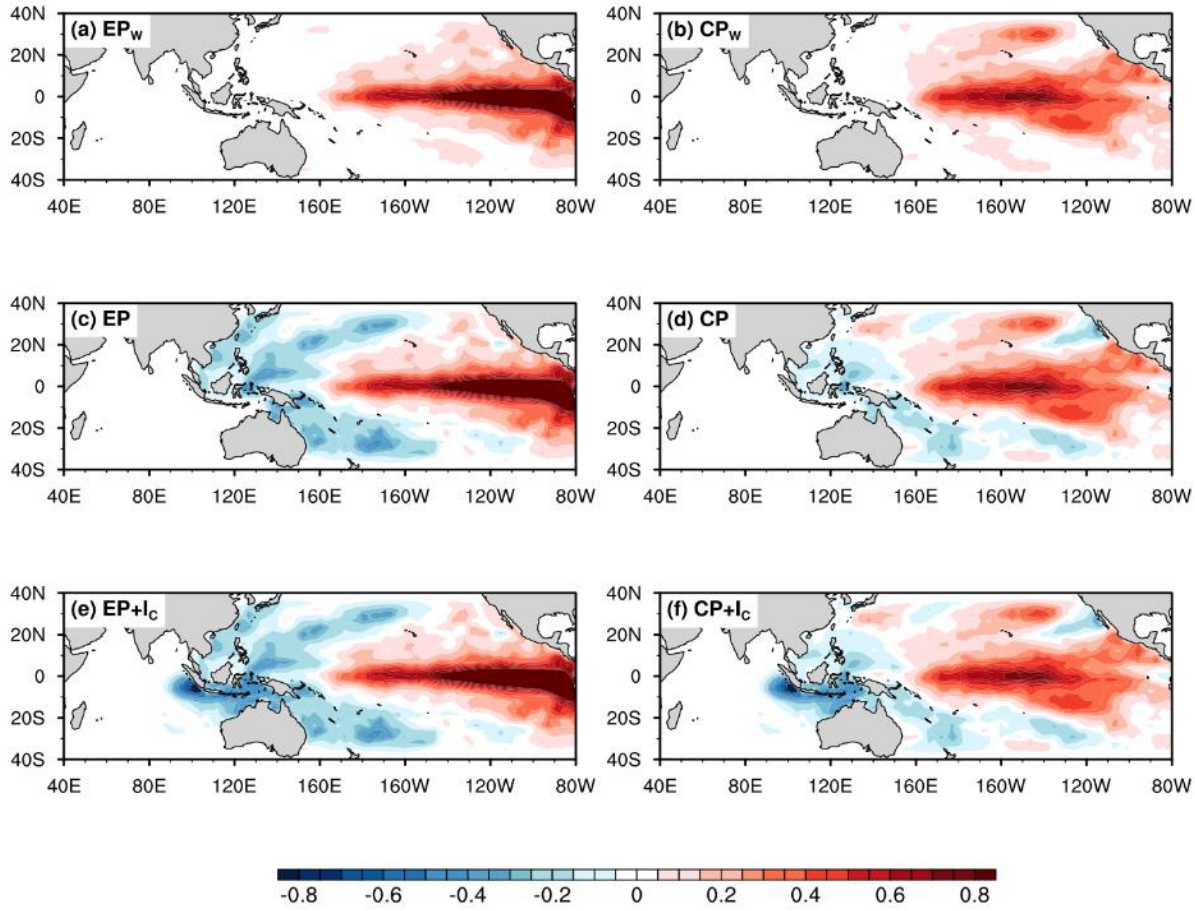


**Figure 1.** The JJAS mean composites of SST anomalies overlaid with SST climatology to provide surface forcing in IGCM model experiments for EP, CP. In our naming convention, EP and CP suggest whole Pacific-basin SST anomalies, while W and C subscripts indicate experiments in which only the warm or cold SST anomalies are retained (respectively) for El Niño (over Pacific Ocean) and IOD (over Indian Ocean) events.

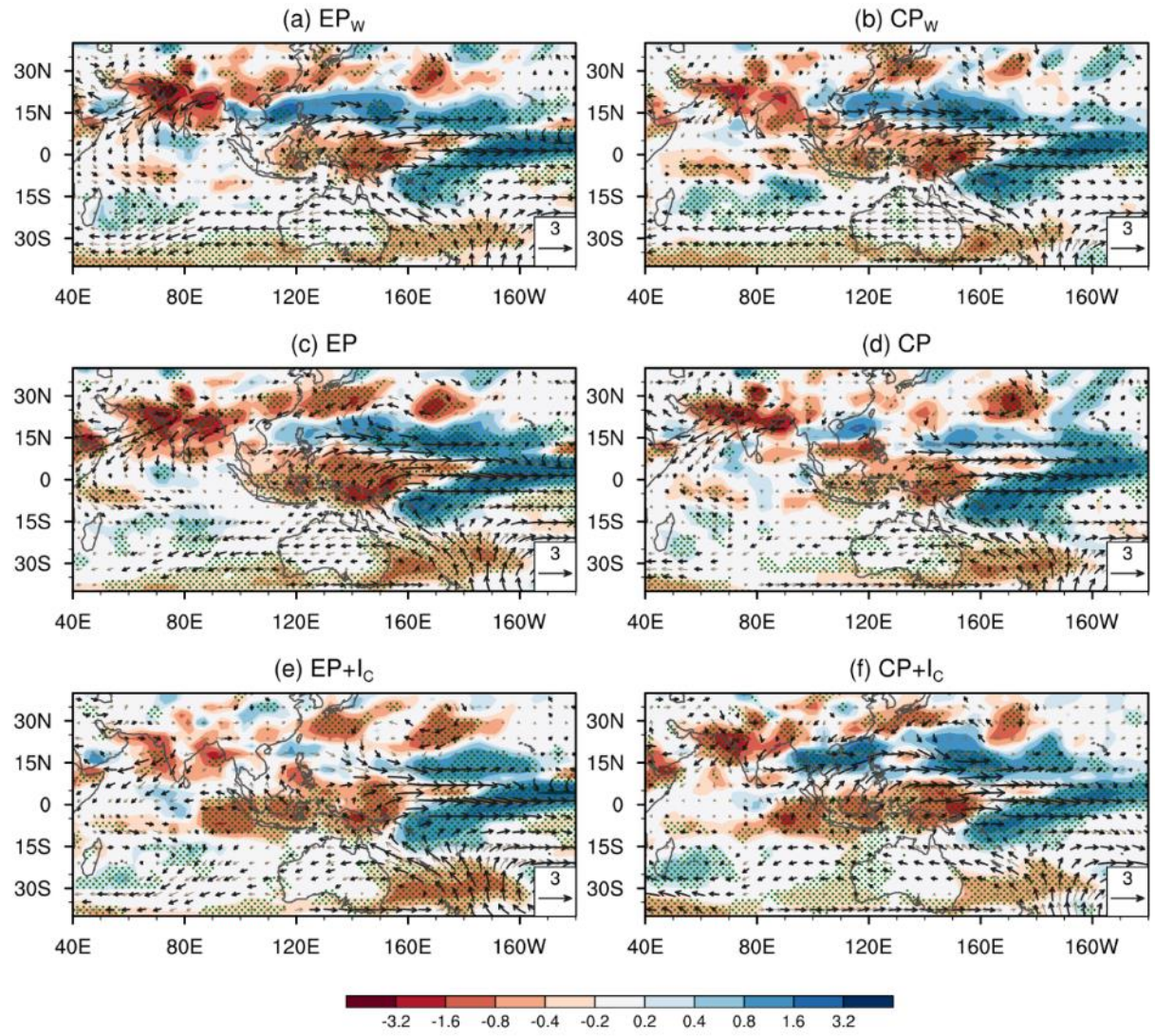


516

517

518 **Figure 2.** IGCM responses in JJAS rainfall (shaded, mm $d^{-1}$) and circulation (850 hPa wind
519 vectors; m $s^{-1}$) over the ISM domain for the 6 model experiments shown in Figure 1. (**a-b**) the
520 model response to Pacific warm SST forcing only ($EP_W$, $CP_W$); **(c-d)** model response to whole-
521 basin SST forcing (EP, CP); **(e-f)** model response to EP, CP SSTs combined with cold Indian
522 Ocean SST anomalies associated with IOD events ($EP+I_C$, $CP+I_C$). The wind vectors (black) and
523 the precipitation (hatched) represent statistical significance at the 90% confidence level based on
524 a student's t-test.

525

526

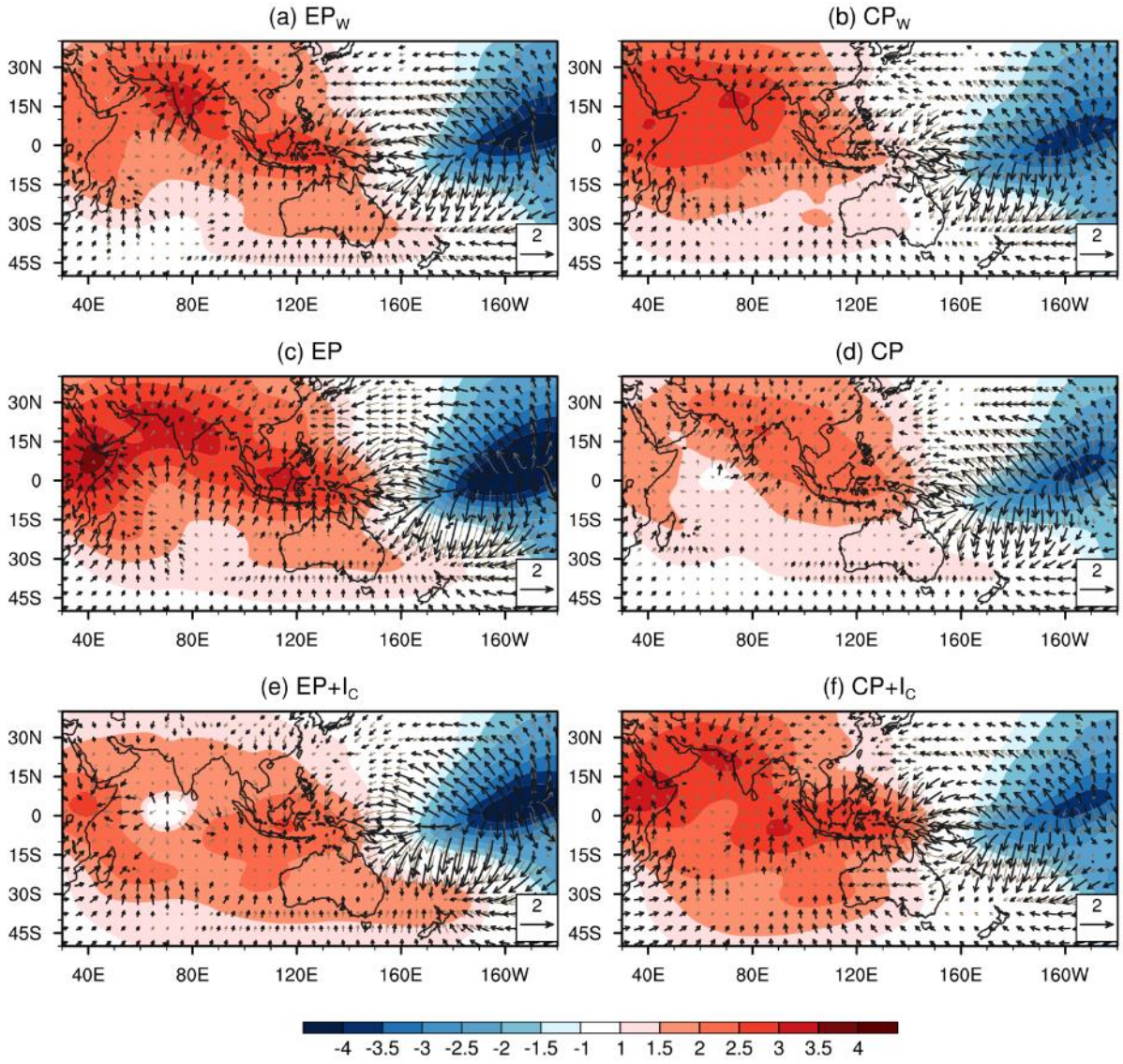


**Figure 3.** Same as Figure 2, but for upper level (200 hPa) velocity potential (shaded; $10^{-6}$, $m^2\ s^{-1}$) overlaid with divergent wind anomalies (vectors). Only signals of velocity potential significant at the 90% level are shown (shaded), while divergent winds are shaded grey (black) below (above) this level.

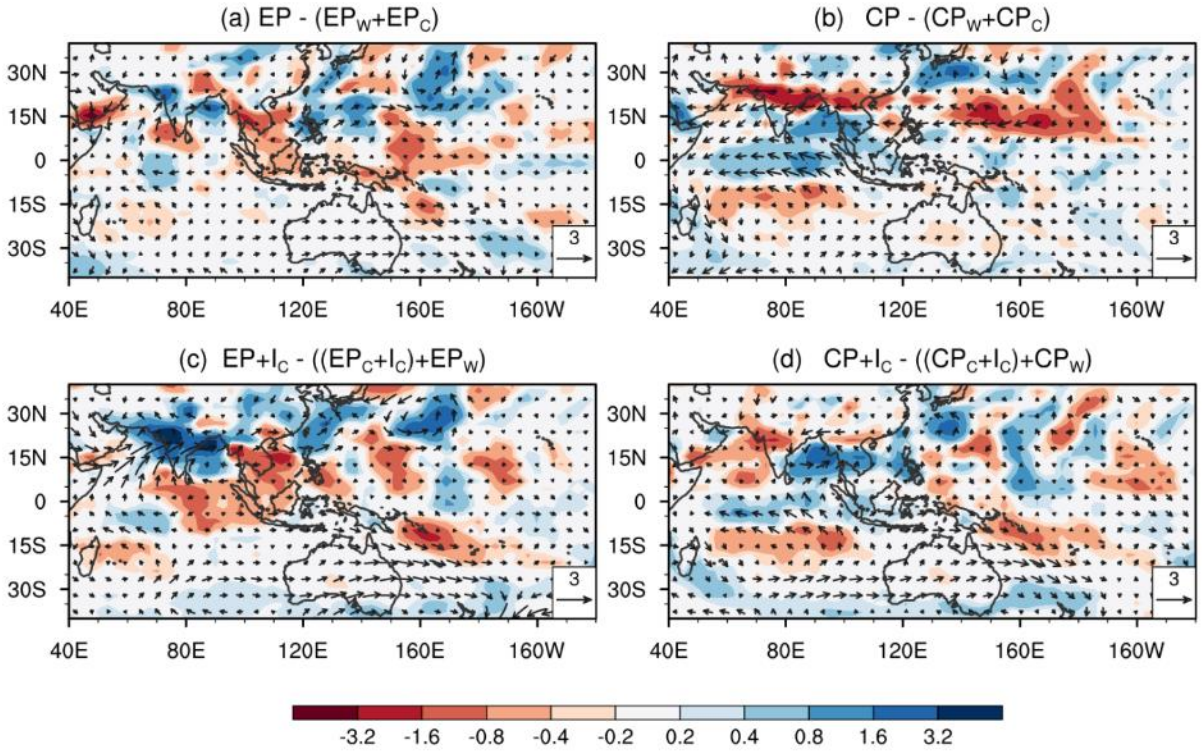


**Figure 4.** Non-linearity in IGCM responses to SST forcing during JJAS, (a-b) rainfall (shaded, mm $d^{-1}$) and circulation (850 hPa wind vectors; m $s^{-1}$) responses between EP (CP) and the sum of responses to $EP_W$ and $EP_C$ ($CP_W$ and $CP_C$), (c-d) between EP+$I_C$ (CP+$I_C$) and the sum of responses to $EP_W$ and $EP_C$+$I_C$ ($CP_W$ and $CP_C$+$I_C$).

## Tables

**Table 1**: The list of model experiments. In our naming convention, EP and CP suggest whole Pacific basin SST anomalies, while 'W' and 'C' subscripts indicate experiments where only the warm or cold SST anomalies are retained (respectively) for El Niño (over Pacific Ocean) and IOD (over Indian Ocean) events.

| **Experiments** | **SST forcing** |
|---|---|
| Control (Ctrl) | Monthly SST climatology |
| $EP_W$, $CP_W$ | Ctrl + Pacific Warm SST anomalies |
| EP, CP | Ctrl + Pacific Basin SST anomalies |
| $EP+I_C$, $CP+I_C$ | Ctrl + Pacific Basin + IOD Cold SST anomalies |